

A new parametrization of turbulent orographic form drag

Anton Beljaars, Andrew Brown¹
and Nigel Wood¹

Research Department

¹ Met Office, UK

November 2003

*This paper has not been published and should be regarded as an Internal Report from ECMWF.
Permission to quote from it should be obtained from the ECMWF.*



European Centre for Medium-Range Weather Forecasts
Europäisches Zentrum für mittelfristige Wettervorhersage
Centre européen pour les prévisions météorologiques à moyen terme

Series: ECMWF Technical Memoranda

A full list of ECMWF Publications can be found on our web site under:

<http://www.ecmwf.int/publications/>

Contact: library@ecmwf.int

©Copyright 2003

European Centre for Medium Range Weather Forecasts
Shinfield Park, Reading, RG2 9AX, England

Literary and scientific copyrights belong to ECMWF and are reserved in all countries. This publication is not to be reprinted or translated in whole or in part without the written permission of the Director. Appropriate non-commercial use will normally be granted under the condition that reference is made to ECMWF.

The information within this publication is given in good faith and considered to be true, but ECMWF accepts no liability for error, omission and for loss or damage arising from its use.

Abstract

A new parametrization is presented for the representation in large scale models of turbulent form drag due to subgrid orography with horizontal scales shorter than around 5 km. The scheme is based on earlier work in which surface stress and its vertical distribution is formulated in terms of a slope parameter for sinusoidal hills. The new elements of the current parametrization are: (i) the spectrum of the orography is represented by a piecewise empirical power law, (ii) the turbulent form drag scheme integrates over the spectral orography to represent all the relevant scales, and (iii) the wind forcing level of the drag scheme depends on the horizontal scale of the orography, which implies that the smaller scales respond to lighter winds than do the larger scales.

The scheme is controlled by a single parameter, namely the spectral density of the orography at scales of a few km, as can be accurately obtained from a global 1 km data set. The empirical orographic power law spectrum is derived by analysing fine resolution data as available for the USA. In order to be applicable in a large scale model, simplifications are applied. Single column simulations are performed to assess the consequences of these simplifications. Comparisons of single column simulations with output from fine scale simulations for sinusoidal hills show that the approximations are within the uncertainty of the fine scale models. Furthermore, it is felt that the scheme is sufficiently accurate given the uncertainty in the characterization of the orography with current global data sets.

1 Introduction

Subgrid scale orography is an important contributor to surface drag in large scale models. Drag can be related to gravity waves, blocking of the low level flow or to turbulent drag due to the form drag exerted by the subgrid obstacles. Typically, parametrizations of each of these processes coexist in large scale models without any explicit interaction. This is an approximation to reality since there is no spectral gap in the scales of the orography that contribute to each process. However, a workshop on orography (ECMWF 1997) recommended using the subgrid scales above 5 km for the gravity wave and low level blocking parametrizations (e.g. as in Lott and Miller 1996) and to use the scales below 5 km for the turbulent effects. Vertical propagation of gravity waves becomes impossible at small horizontal scales and 5 km was considered to be a reasonable limit. This paper focuses on turbulent form drag due to scales smaller than 5 km.

In the ECMWF numerical weather prediction (NWP) model, the so-called effective roughness length concept is used which means that in areas with orography, the roughness length is enhanced above its vegetative value with the aim that the correct total surface drag (due to the sum of turbulent shear stresses and pressure forces) should be obtained (Taylor et al. 1989; Mason 1991; Wood and Mason 1993, hereafter WM93). The concept is justified by, for example, observations, well above the orographic features, of a logarithmic profile with a slope that scales with the total surface drag (Grant and Mason 1990). The turbulent form drag due to sub-grid orography can be substantial and therefore the effective roughness lengths can be very large. To avoid numerical problems, the roughness lengths are limited to be no greater than 100 m in the ECMWF system. Since the transfer of heat and moisture between the lowest model level and the surface is hardly affected by sub-grid orography effects, the roughness lengths for heat and moisture are reduced in these areas in order to compensate for the orographic enhancement in the aerodynamic roughness length (Hewer and Wood 1995).

The introduction of effective roughness lengths led to significant improvements in the performance of a number of NWP models (e.g. Milton and Wilson 1996). However, the concept does have a number of disadvantages. These include spuriously low, low-level wind speeds in regions of high effective roughness, the rather circuitous approach required to the parametrization of the scalar fluxes, and difficulties in understanding the interactions of the scheme with stability and with orographic gravity wave drag and flow blocking schemes. In view of these concerns, Wood et al. (2001), hereafter WBH01, propose a scheme in which the effects of turbulent form drag on subgrid orography are represented by an explicit orographic stress profile. However, they consider only the

simple case of flow over an infinite series of sinusoidal ridges, and do not address the key issue, for large-scale models, of the characterization of complex, real orography containing multiple scales.

One major problem for the large-scale models is the lack of global orographic data at sufficiently high resolution. For turbulent orographic form drag, the horizontal scales of interest are those of around 5 km down to say 10 m and the most relevant parameter is slope (e.g. WM93). This puts the emphasis on the high wave number part of the spectrum. A popular data source in the global modelling community is the GTOPO30 data set at 30" (about 1 km) resolution (Gesch and Larson 1998). In spite of the high resolution, the data is not fine scale enough to derive a slope parameter at the required scales. Many modelling centres derive the slope from what is available but the result is obviously highly dependent on the resolution of the orographic data, which is not very satisfactory. As long as topographic data at higher resolution is missing on a global scale, it is necessary to parametrize the missing part of the spectrum in terms of parameters that can be resolved by the available data. For instance, in the UK Met Office model, an empirical link is made between variance at larger scales and the silhouette slope parameter at smaller scales based on fine scale orographic data for limited areas (Milton and Wilson 1996).

Even if extremely high resolution data were available, slope parameters (e.g. variance of the slope or the silhouette parameter as proposed by Mason 1991) commonly used in the calculation of effective roughness lengths have the problem that they do not necessarily asymptote for infinitely fine orographic resolution. For the variance of the slope to converge, the orographic power spectrum has to be steeper than k^{-3} (where k is wave number). Real orography tends to have power spectra with slopes between -1 and -4 (see Uhrner 2001) and thus this condition may not be met. A possible reason for the apparently potentially unlimited roughness length and drag coefficient is that the calculation has not taken into account the different appropriate wind forcing levels for the different scales (P.A. Taylor, personal communication). The small-scale features should 'feel' the wind from lower in the boundary layer than the larger scales, and thus contribute less drag.

The aim of the present paper is to build on WBH01 and develop a scheme which addresses some of these issues, and which is suitable for practical application in a large-scale model. The main steps are as follows:

1. In section 2 an analysis is made of the spectral characteristics of orography in the USA from a 3" (about 100 m) resolution data set. It is used to develop a parametrization of the orographic spectrum which takes as an input data which can be obtained from the 30" GTOPO data set which covers the whole globe.
2. The new turbulent orographic form drag formulation is presented in sections 3a-3d. For each wave number it is based on the surface drag formulation of WM93 (with some simplifications) and uses the WBH01 distributed drag formulation. It then integrates over the orographic spectrum to obtain the contribution from all scales. Note that, in order to address the convergence issue described above, the height of the wind forcing level is made part of the integral over the wave number spectrum of orography.
3. Further simplifications to allow an efficient implicit implementation are described in section 3e.
4. In section 4, single column model simulations are used to assess the consequences of the simplifications made. The impact of vertical resolution (which can be relatively coarse in large-scale models) is also addressed.

2 Spectral characteristics of small scale orography

The spectral characteristics of topography as presented by different studies vary substantially (Young and Pielke 1983; Bannon and Yuhua 1990; Mengesha 2001; Uhrner 2001). However, most studies cover only a limited area in a particular location, so it is difficult to generalize the results.

Here the small scale orography is characterized by using the digital elevation data from the U.S. Geological Survey at 3 arc second (about 100 m North-South and less East-West) resolution. The data comes in $1 \times 1^\circ$ areas as 1200×1200 points and covers the USA (about 900 areas). For each of these areas the one dimensional spectrum is computed in the East-West direction as well as in the North-South direction. To obtain a statistically more reliable estimate, spectra from the different cross sections in the same direction are averaged. An example of 6 slope spectra (spectral density multiplied by k^2) is given in Fig. 1. A number of points are worth noting:

- The spectra have a clear aliasing tail at high wave numbers, which is an artefact of the way the orography has been sampled. The spectra are only realistic to about $k = 0.015 \text{ m}^{-1}$ for the East-West spectra and to about $k = 0.012 \text{ m}^{-1}$ for the North-South spectra. (This is a negligible difference and henceforth the smaller limit, $k = 0.012 \text{ m}^{-1}$, will be used for both spectra.)
- There is a rather distinct change in slope at about wave number $k = 0.003 \text{ m}^{-1}$. The position of the scale break varies but inspection of about 40 spectra does not indicate any systematic variation with e.g. height of the mountains.
- Most spectra can be represented reasonably well by a piecewise linear fit in the wave number ranges from 0.0002 to 0.003 and from 0.003 to 0.012 m^{-1} .

A spectral analysis was made for all the available $1 \times 1^\circ$ areas over the USA and a linear fit was made (on a logarithmic scale) in two spectral bands, with the spectra characterized by parameters a_1, n_1, a_2, a_2 as follows

$$\begin{aligned} F_o(k) &= a_1 k^{n_1} \text{ for } 0.0002 < k < 0.003 \text{ m}^{-1}, \\ F_o(k) &= a_2 k^{n_2} \text{ for } 0.003 < k < 0.012 \text{ m}^{-1}. \end{aligned} \quad (1)$$

The spectral intensity at wave number $k = 0.001 \text{ m}^{-1}$ (i.e. $a_1 (0.001)^{n_1}$) of the linear fit in the low wave number band is used as a measure for the amplitude of the small scale orography.

First, it is verified that the East-West spectra and the North-South spectra do not behave differently. Indeed the spectral amplitudes as well as the slopes of the spectra show high correlation between the two directions and the scatter is fairly small (Figs. 2 and 3). Although distinct directionality has been reported for particular areas (e.g. for the Sandhills in Nebraska, Mengesha et al. 2001), it is concluded that, for most areas, the directional effects are only second order.

From Figs. 2 and 3 it is clear that the spectral slope in the two bands is typically rather different, although the scatter within each band is large, implying a substantial variation of spectral shape from one location to the other. Conceivably the spectral slope might be a function of the amplitude of the small scale orography. However, Fig. 4 shows that this dependence is weak (compared to the scatter) and it will therefore be neglected. Accordingly, we simply take the average power law exponents in each of the two wave number bands as follows

$$\begin{aligned} n_1 &= -1.9 \text{ for } 0.0002 < k < 0.003 \text{ m}^{-1}, \\ n_2 &= -2.8 \text{ for } 0.003 < k < 0.012 \text{ m}^{-1}. \end{aligned} \quad (2)$$

With the above assumption about the shape of the spectrum, there is only one parameter left that needs to be derived from the global orographic set, namely a_1 . This parameter is determined by filtering the scales between 3 km and 22 km and determining the standard deviation of the terrain height in this scale range (see Appendix A for a discussion on the selection of parameters). A global 1 km data set is sufficient now to determine this parameter. In appendix A, a filter is defined for this purpose. The characteristic wave number of the filter is

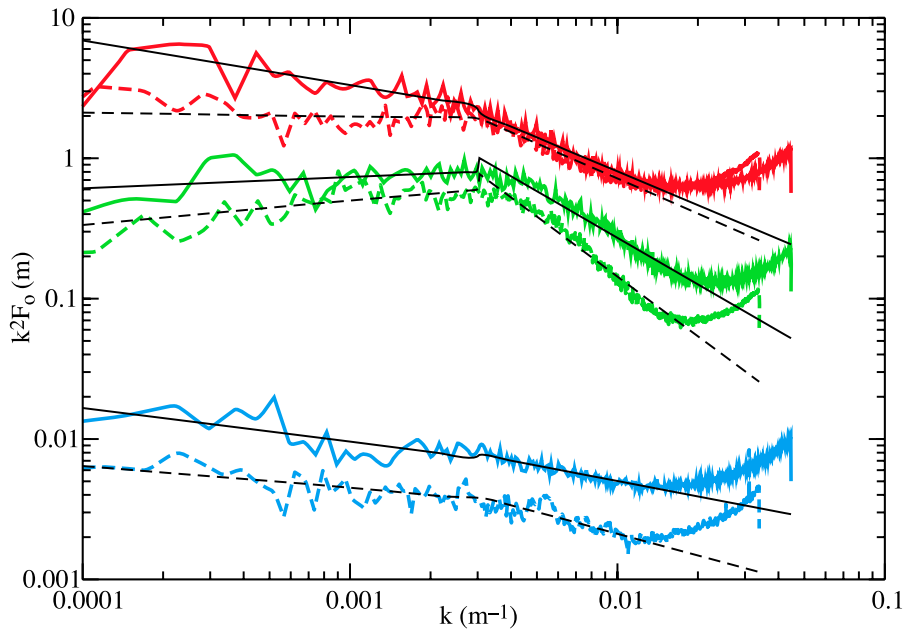


Figure 1: Examples of slope spectra from 3" data in $1 \times 1^\circ$ areas. The thin lines represent the fit in the wave number bands from 0.0002 to 0.003 and from 0.003 to 0.012 m^{-1} . The top, middle and bottom pair of curves are for "Adel-e", "Ajo-e" and "Aberdeen-e" respectively (names given to the area by USGS). The curves fitted by the solid line are for the E-W direction, and the curves fitted by the dashed lines are for the N-S direction.

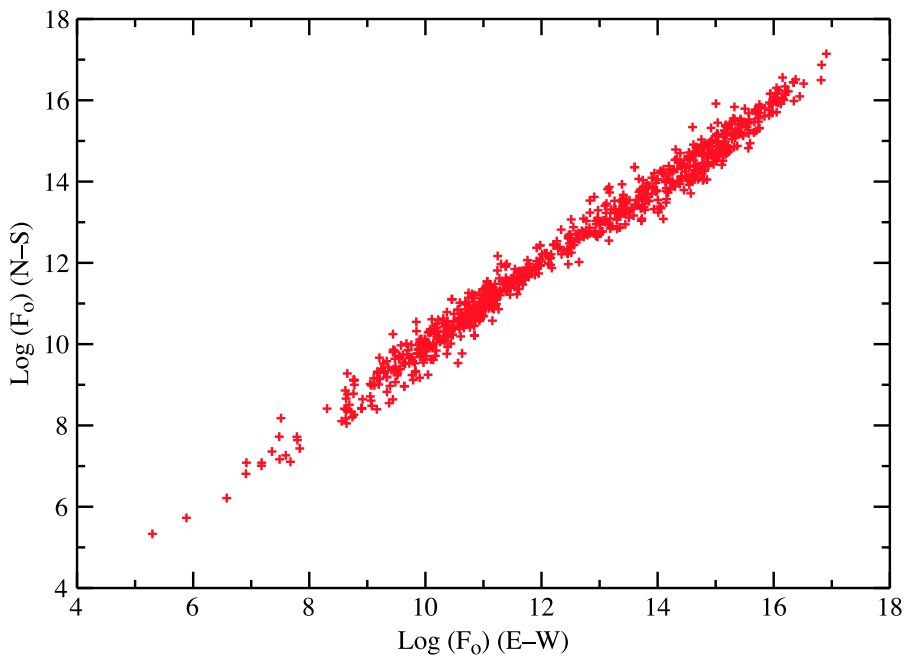


Figure 2: The logarithm of spectral density F_0 (m^3) at wave number $k = 0.001 m^{-1}$ in the North-South direction (ordinate) versus the logarithm of spectral density of the same area in the East-West direction (abscissa). Each point represents a $1 \times 1^\circ$ area.

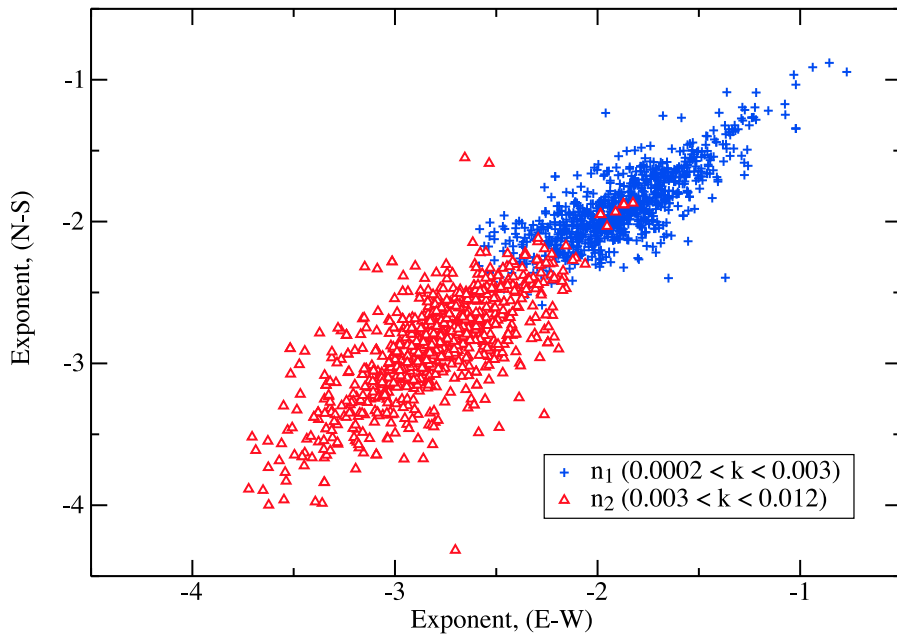


Figure 3: The exponent of the power law of the North-South spectrum versus the exponent of the East-West spectrum of the same area. Two wave number bands are distinguished. Each point represents a $1 \times 1^\circ$ area.

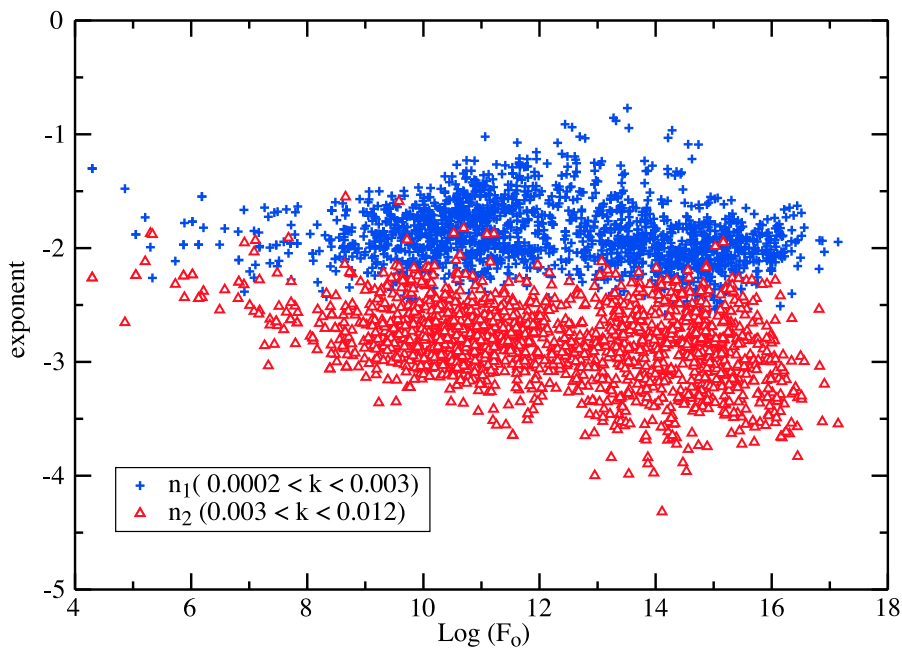


Figure 4: The exponent of the power law of the spectrum as a function of the spectral density F_0 (m^3) at wave number $k = 0.001 \text{ m}^{-1}$ of the same area. Two wave number bands are distinguished. Each point represents a $1 \times 1^\circ$ area.

$k_{flt} = 0.00035 \text{ m}^{-1}$ and the constants a_1 and a_2 in (1) are linked to the filtered variance σ_{flt}^2 in the following way:

$$\begin{aligned} a_1 &= \frac{\sigma_{flt}^2}{I_H k_{flt}^{n_1}}, \quad a_2 = a_1 k_1^{n_1 - n_2}, \\ n_1 &= -1.9, \quad n_2 = -2.8, \quad I_H = 0.00102 \text{ m}^{-1}, \\ k_{flt} &= 0.00035 \text{ m}^{-1}, \quad k_1 = 0.003 \text{ m}^{-1}. \end{aligned} \quad (3)$$

3 Turbulent orographic drag parametrization

As noted in the introduction, most large-scale models use the effective roughness length concept. In this approach an estimate of the pressure drag is combined with one of the turbulent drag over the flat terrain to define an effective roughness length. Here, the two drag components are kept separate and both are implemented in the vertical diffusion scheme with implicit numerics.

Before describing the new formulation, the WM93 parametrization for the surface pressure drag is summarized and simplified in the following two subsections. Then the WBH01 study is used to distribute the drag in the vertical (subsection 3c) and the new formulation is described for a continuous range of scales (subsection 3d). Finally, further simplification to allow an efficient implicit implementation is described in subsection 3e.

3.1 The Wood and Mason parametrization

WM93 propose a scheme for the effective roughness length that unifies gentle topography (Taylor et al. 1989) and steep topography (Mason 1985). Here only the pressure drag is considered and it is simplified to make it suitable for a large scale model. The turbulent orographic drag according to WM93 can be expressed as:

$$|\vec{\tau}_{os}|/\rho = \alpha\beta\pi^2 \frac{u_{*o}^2}{|\vec{U}(h_m)|^2} \frac{A}{S_h} \frac{A}{S_d} |\vec{U}(z_m)|^2, \quad (4)$$

where $|\tau_{os}|$ is the pressure force per unit area (stress) in the direction of the mean wind, ρ is air density, α is a shear dependent parameter, β is a shape factor (1 for two-dimensional hills), u_{*o} is the friction velocity of the unperturbed flow, A is the frontal or silhouette area of the topography accumulated over horizontal domain of area S_d , and S_h is the base area of the topography. Since here mountainous terrain is considered rather than isolated hills, S_h is set to S_d . Parameter $(A/S_d)^2$ is equal to the mean square of the slope which is $2\bar{\theta}^2/\pi^2$ for sinusoidal topography ($\bar{\theta}^2$ is the variance of the slope). Length scales h_m and l are defined in WM93 starting from a horizontal length scale λ (wave length for sinusoidal topography) and peak to valley amplitude h ($A/S_d = h/\lambda$ for a sinusoidal mountain) by:

$$\begin{aligned} h_m \log^{1/2} \left(\frac{h_m}{z_o} \right) &= \frac{1}{4} \lambda, \\ l \log \left(\frac{l}{z_o} \right) &= \frac{1}{2} \kappa^2 \lambda, \\ z_m &= h_m \quad \text{for } h \leq h_m, \\ z_m &= h \quad \text{for } h > h_m. \end{aligned} \quad (5)$$

The functional form of the shear dependent coefficient α , is the subject of some debate and depends on the level of turbulent closure employed. Belcher et al. (1993) give the linear form for a second-order closure while

WM93 give the form appropriate for a first-order closure. Since here results of the proposed parametrization are later compared with a first-order closure model, the form proposed by WM93 is used, namely:

$$\alpha = 2 \left(\frac{\log(h_m/z_o)}{\log(l/z_o)} \right)^4 + \log(l/z_o). \quad (6)$$

3.2 Simplified formulation

The WM93 formulation was developed using fine scale simulations of idealized topography, basically two- and three-dimensional sinusoidal cases. Later, contributions from different wave numbers will be integrated to obtain the total effect of a broad spectrum of scales. To be able to do so, it is necessary to have a very simple formulation for a single wave number. In the WM93 scheme, a number of parameters are only weakly dependent on the dimensions of the topography. To simplify, these parameters are assumed here to be constant:

$$\begin{aligned} \alpha &= 12, \beta = 1, \\ z_m &= h_m, \\ h_m &= c_m \lambda \text{ with } c_m = 0.1, \\ C_{md} &= \frac{\kappa^2}{\log(h_m/z_o)} = 0.005. \end{aligned} \quad (7)$$

The resulting simplified expression for the orographic stress is

$$|\vec{\tau}_{os}|/\rho = 2 \alpha \beta C_{md} \bar{\theta}^2 |\vec{U}(h_m)|^2. \quad (8)$$

Expression (8) is a rather drastic simplification of (4) and not all underlying assumptions are justifiable. Equation (8) is quadratic in slope θ and uses velocity at height h_m , which applies to the low slope approximation of Taylor et al. (1993). The steep slope formula by Mason (1985) is linear in θ and uses $U(h)$ as a velocity scale. WM93 is quadratic in θ also for steep slopes, but compensates with the $U^2(h)/U^2(h_m)$ term. Equation (8) has the compensation by using the velocity at height h_m rather than at height h . By having h_m , the dependence is on the horizontal scale rather than on the vertical scale h , which is required for the spectral integral later which does not have information about h . There is no a priori indication that this simplification is adequate but single column simulations, presented later, indicate how good it is.

3.3 The Wood, Brown and Hewer formulation of turbulent orographic drag

WBH01 use the WM93 formulation for the orographic contribution to the surface drag, but do not convert the drag into an effective roughness length. Instead, they suggest a prescribed distribution of the drag with height and apply it directly as a flux divergence term in the momentum equations of their single column model. An exponential distribution is proposed with a vertical decay scale l_w :

$$\vec{\tau}_o(z) = \vec{\tau}_{os} e^{-z/l_w}. \quad (9)$$

WBH01 use a vertical decay scale of $l_w = \lambda/\pi = 2/k$ and cap it by $z_i/3$ where z_i is the boundary layer depth. They consider only cases with a single wave number. The use of their scheme for real cases with a continuous range of scales is considered in the next subsection.

3.4 A new formulation for a continuous range of scales

The variance of the slope $\bar{\theta}^2$ can be written as an integral over the orographic spectrum

$$\bar{\theta}^2 = \int_{k_o}^{\infty} k^2 F_o(k) dk, \quad k_o = 0.000628 \text{ m}^{-1}, \quad (10)$$

where $k (= 2\pi/\lambda)$ is the wave number, k_o , the lower bound of the integral, is set to half a wave length of 5 km, and $F_o(k)$ is the variance spectrum of the orography. Since h_m in (8) is assumed to be inversely proportional to wave number (the reference level for wind forcing of the drag scales with the horizontal wave length of the hill), it is plausible to assume that for a continuous spectrum (8) can be written as

$$|\vec{\tau}_{os}|/\rho = 2\alpha\beta C_{md} \int_{k_o}^{\infty} k^2 F_o(k) |\vec{U}(2\pi c_m/k)|^2 dk. \quad (11)$$

The integral can be interpreted as a superposition of contributions from different wave numbers to the orographic form drag (with no phase information). As such it may appear as an approximation that only applies for small amplitudes in a linear flow regime. However, the integral may also be looked at as an empirical way to generate a slope parameter (with some additional scaling for the forcing level) which is applied to an empirical drag law. This is the WM93 drag law which applies to gentle as well as steep hills with flow separation. Therefore, while the scheme is linear in that it neglects interactions between wave numbers, it is non-linear in its response to the steepness of different wave numbers.

Similar to (11) for the stress divergence from (9) it is postulated that

$$\frac{\partial}{\partial z} \vec{\tau}_{os}/\rho = -2\alpha\beta C_{md} \int_{k_o}^{\infty} \frac{k^2}{l_w} F_o(k) |\vec{U}(2\pi c_m/k)| |\vec{U}(2\pi c_m/k)| e^{-z/l_w} dk, \quad (12)$$

with $l_w = \min(2/k, 2/k_1)$.

The equation is written in vector form now because the stress divergence extends well above the surface layer and so the wind turning is likely to be non-negligible. Note that in order to limit the number of independent length scales, the maximum value of the decay scale has been set to $2/k_1$ where $k_1 = 0.003 \text{ m}^{-1}$ is the wave number at which the spectrum changes slope. While WBH01 advocate the use of $z_i/3$ as the maximum scale, they note that their results are not very sensitive to this choice, and thus the impact of this simplification is likely to be small.

Equation (12) has a number of attractive features. First, the equation reduces to the simplified WM93 and WBH01 parametrizations for sinusoidal hills because $F_o(k)$ is a delta function for these situations. Second, each wave number has its own scale-dependent wind forcing level. High k values (short waves) have a low forcing level. This feature alleviates the convergence problem for high wave numbers as the wind speed decreases near the surface. And third, the vertical decay scale is wave number dependent. Hence the flux divergence of the short waves covers a shallow depth whereas the flux divergence of the longer waves is over a deep layer. This will further tend to reduce the contribution to the drag of the small scales, as they will be relatively efficient at decelerating low-level wind (which will impact both on parametrized form drag and on the non-orographic turbulent drag). The feedback of the drag on the flow is an important feature of the scheme, because it leads to sheltering of the small scales by the larger scales: through their drag, the large scales reduce the wind near the surface which is used as the forcing level for the small scales (see Hara and Belcher 2002, for a discussion of these effects for wind generated ocean waves).

An example of how the different wave numbers contribute to the integral in (11) is given in Fig. 5. The integrand of the integral multiplied by k (to compensate for the distortion of the logarithmic axis) is plotted as a function of the wave number together with $|\vec{U}(2\pi c_m/k)|^2$. The velocity profile has been taken from a single

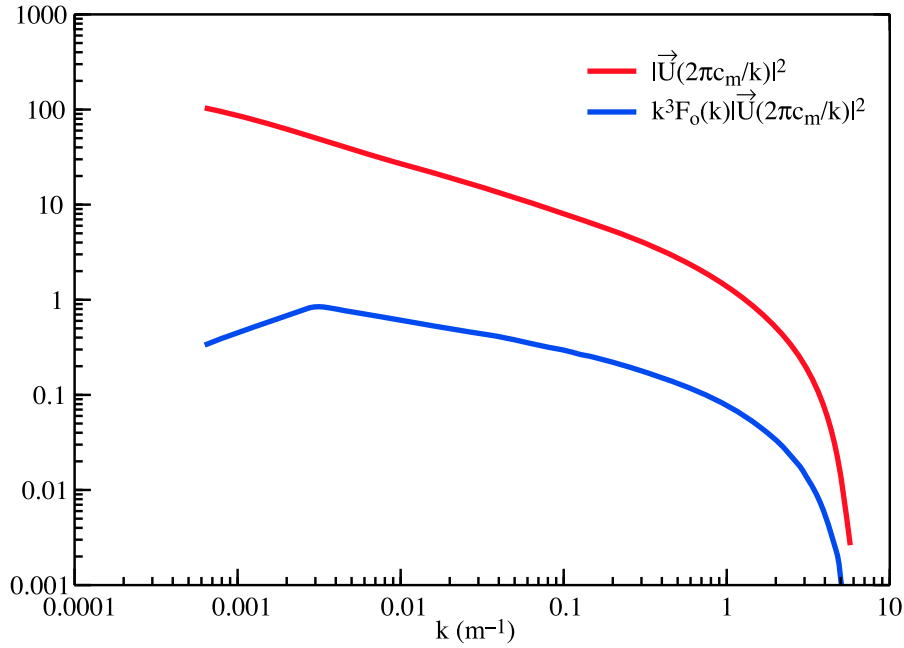


Figure 5: Integrand of (11) multiplied by k (to compensate for the distortion of the logarithmic axis) as a function of wave number k (dashed). The profile of $|\vec{U}(2\pi c_m/k)|^2$ is also shown (solid). The velocity profile has been taken from a single column simulation with $z_o = 0.1$ m and $\sigma_{flt} = 200$ m.

column simulation with $z_o = 0.1$ m and $\sigma_{flt} = 200$ m (the single column model results are presented in the next section). It is clear that the velocity part of the integrand is responsible for the decay of the integrand at high wave numbers. Without the velocity as part of the integrand, the integral would not converge.

3.5 Further simplifications for efficient implicit implementation

The main disadvantage of (12) is that the local stress divergence depends on values of U at different heights. This makes an implicit formulation of the scheme (which is essential for practical application in an NWP model) very difficult, as the diagonal structure of the implicit solver is lost. Here a simplification is developed which involves taking the velocity term out of the integral and regains the diagonal structure.

To illustrate the behaviour of the integrand in (12), the velocity term and the remaining part (multiplied by k to compensate for the logarithmic distortion) are shown in Fig. 6 for different heights. It is clear that the peak of the remaining part moves to shorter scales (larger k) as z decreases. If it is assumed that U varies only slowly with height then, for each z , it may be taken outside of the integral and set to its value at the wave number at which the remaining part of the integrand has its maximum value. For $k > k_1$ this will occur when $k^3 F_o(k) \exp(-zk/2)$ has a maximum. With $F_o(k) \propto k^{n_2}$, the maximum of this function is at $k_{max} = 2(n_2 + 3)/z$, and hence the level at which to calculate U in (12) is at $z_{max} = 2\pi c_m/k_{max}$. With $n_2 = -2.8$ this gives $z_{max} = 1.57z$ (for $z < 133$ m) i.e. the height to evaluate the wind speed is of the same order of magnitude as the height where the flux divergence is needed. A possible simplification of (12) is therefore

$$\frac{\partial}{\partial z} \vec{\tau}_o / \rho = -2\alpha \beta C_{md} C_{corr} |\vec{U}(z)| \vec{U}(z) \int_{k_o}^{\infty} \frac{k^2}{l_w} F_o(k) e^{-z/l_w} dk, \quad (13)$$

$$l_w = \min(2/k, 2/k_1).$$

This approximation is unlikely to be accurate and therefore an adjustable correction factor C_{corr} has been

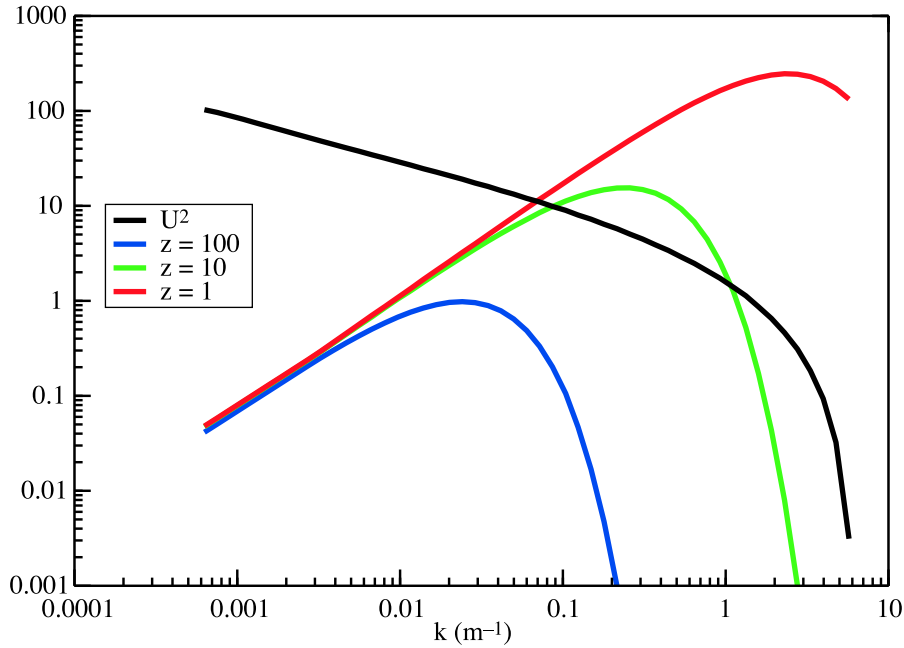


Figure 6: Breakdown of the integrand of (12) multiplied by k (to compensate for the logarithmic distortion) into the velocity part $|\vec{U}(2\pi c_m/k)|^2$ (solid) and the remaining part $(k^3/l_w)F_o(k)\exp(-z/l_w)$ for different values of z (dashed lines).

introduced to improve its accuracy. The correction factor will be optimized by comparing the results of (12) and (13) in single column simulations.

It is recognised that the above derivation of the approximate form (13) is not rigorous. Its primary justification is the empirical observation (see section 4) that it compares well with the full expression (12).

4 Single column simulations

Single column simulation are used to illustrate the behaviour of the parametrization and to optimize the approximation. The model is a simple Ekman layer model with turbulence closure for neutral flow (see Appendix B for a more detailed description). The geostrophic wind is set to 10 ms^{-1} in the x -direction and the initial condition for wind is a logarithmic profile between the specified roughness length and the 500 m level, and equal to the geostrophic wind above 500 m. It is still necessary to specify a roughness length as a surface boundary condition. In this case it represents the vegetation with typical values between 0.01 and 1 m. The top of the model is at 5000 m. The model is integrated for 10 hours which results in a near steady state. All the results shown here, refer to the model state after 10 hours.

Before using orography with a broad spectrum, the single column model will be applied to sinusoidal hills with varying amplitude to investigate the consequences of the simplifications that have been applied to WM93. For sinusoidal orography with a peak to valley amplitude h and wave number k_s , the spectrum is

$$F_o(k) = \frac{1}{8}h^2\delta(k - k_s). \quad (14)$$

With $k_s > k_1$, (12) and (13) reduce to

$$\frac{\partial}{\partial z}\vec{\tau}_o/\rho = -\alpha\beta C_{md}k_s^3\frac{1}{8}h^2|\vec{U}(2\pi c_m/k_s)|\vec{U}(2\pi c_m/k_s)e^{-zk_s/2}, \quad (15)$$

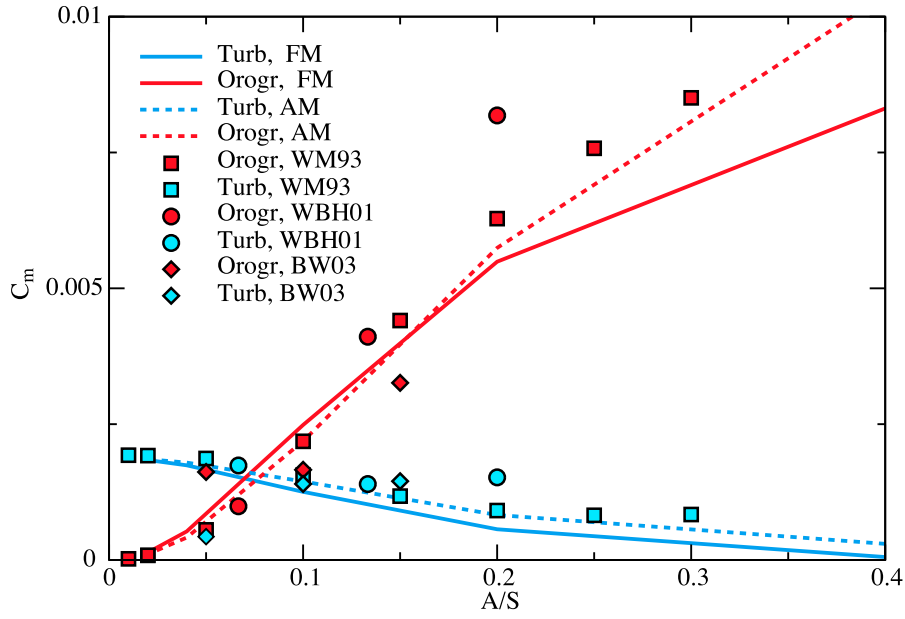


Figure 7: Orographic drag coefficient $|\tau_{os}|/\{\rho U_G^2\}$ (thick lines, solid symbols) and turbulent drag coefficient $|\tau_{ts}|/\{\rho U_G^2\}$ (thin lines and open symbols) from simulations with sinusoidal orography parametrized with (15) (full model, solid lines, denoted FM) and (16) (approximated model with $C_{corr} = 0.6$, dashed lines, denoted AM).

and

$$\frac{\partial}{\partial z} \bar{\tau}_o / \rho = -\alpha \beta C_{md} C_{corr} |\vec{U}(z)| \vec{U}(z) k_s^3 \frac{1}{8} h^2 e^{-zk_s/2}, \quad (16)$$

respectively. The single column model has been integrated for 10 hours with (15) and (16) and a roughness length of 0.1 m. Figure 7 shows the orographic drag coefficient $|\tau_{os}/\rho U_G^2|$ and the turbulent drag coefficient $|\tau_{ts}/\rho U_G^2|$ as a function of A/S . The correction coefficient has been set to 0.6 to obtain a reasonable match over a range of parameter values between the formulations of (15) and (16). The fine scale model results of WM93, WBH01 and Brown and Wood (2003) are also shown. These are all neutral simulations but encompass a range of run lengths, and hill geometries. The differences between (15) and the approximation of (16) are non-negligible, but only of the same magnitude as the differences between fine scale model results. The effect of the approximations in the mathematical formulation is probably less than the uncertainty in a number of other aspects of the parametrization (e.g. characterization of the orography).

Single column simulations are repeated for the full empirical orographic spectrum (as defined through (1) and (3)). Three version of the model are compared:

- *High Resolution and Full Model (HR/FM)*. A logarithmic distribution of 30 model levels is used between the surface roughness and 5000 m, resulting in a 1.45 height ratio between levels (i.e. for $z_o = 0.1$ m, levels at 0.145, 0.210, 0.305, 0.442, 0.641, ... m). The orographic stress divergence is evaluated using (12) and the integral in this equation is evaluated at all model levels every time step.
- *High Resolution and Approximated Model (HR/AM)*. Same as above except that the stress divergence is evaluated using (13) i.e. the integral depends on z only and does not depend on the wind profile.
- *ECMWF model Resolution and Approximated Model (ER/AM)*. Instead of the logarithmic distribution of grid points, the ECMWF model levels are used (23 levels up to 5000 m). The main difference is near the surface; the lowest model levels are at 10, 30, 60, 103, 163, 240, 337, 456 ... m.

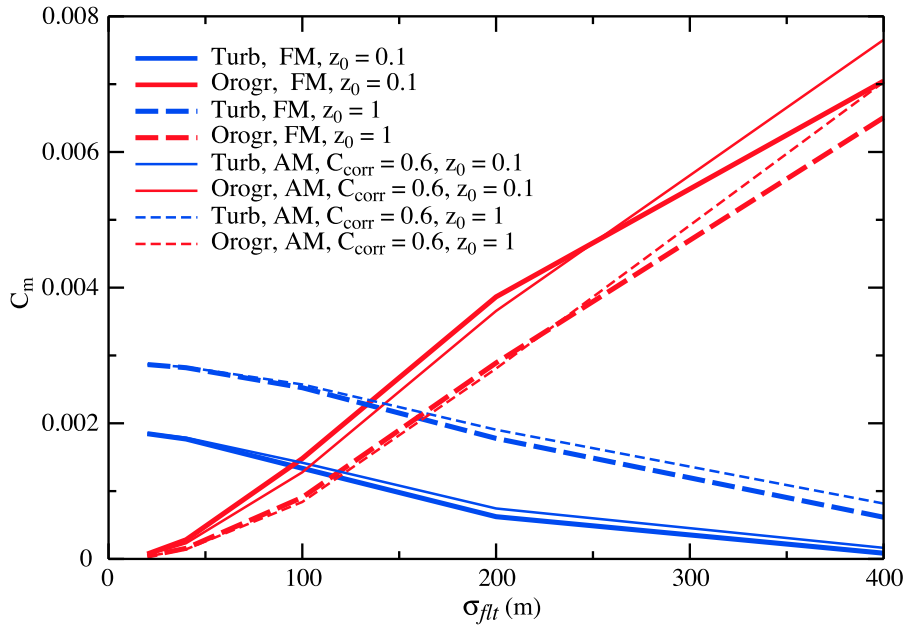


Figure 8: Orographic and turbulent drag coefficients as a function of the standard deviation of the filtered subgrid orography (σ_{flt}) from the full model (FM), and the approximation (AM) with $C_{corr} = 0.6$.

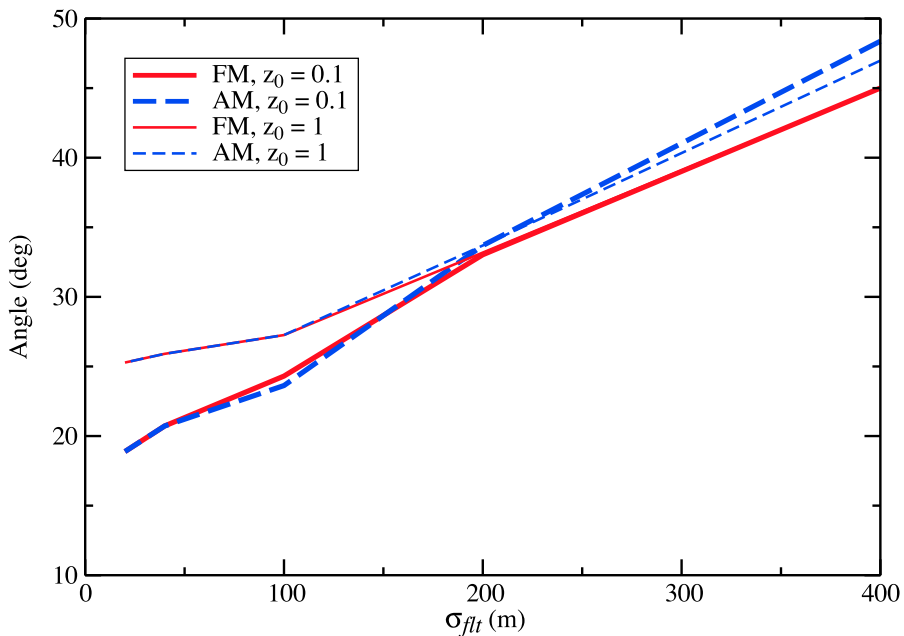


Figure 9: Ageostrophic angle of surface wind as a function of the standard deviation of the filtered subgrid orography (σ_{flt}) from the full model (FM), and the approximation (AM) with $C_{corr} = 0.6$.

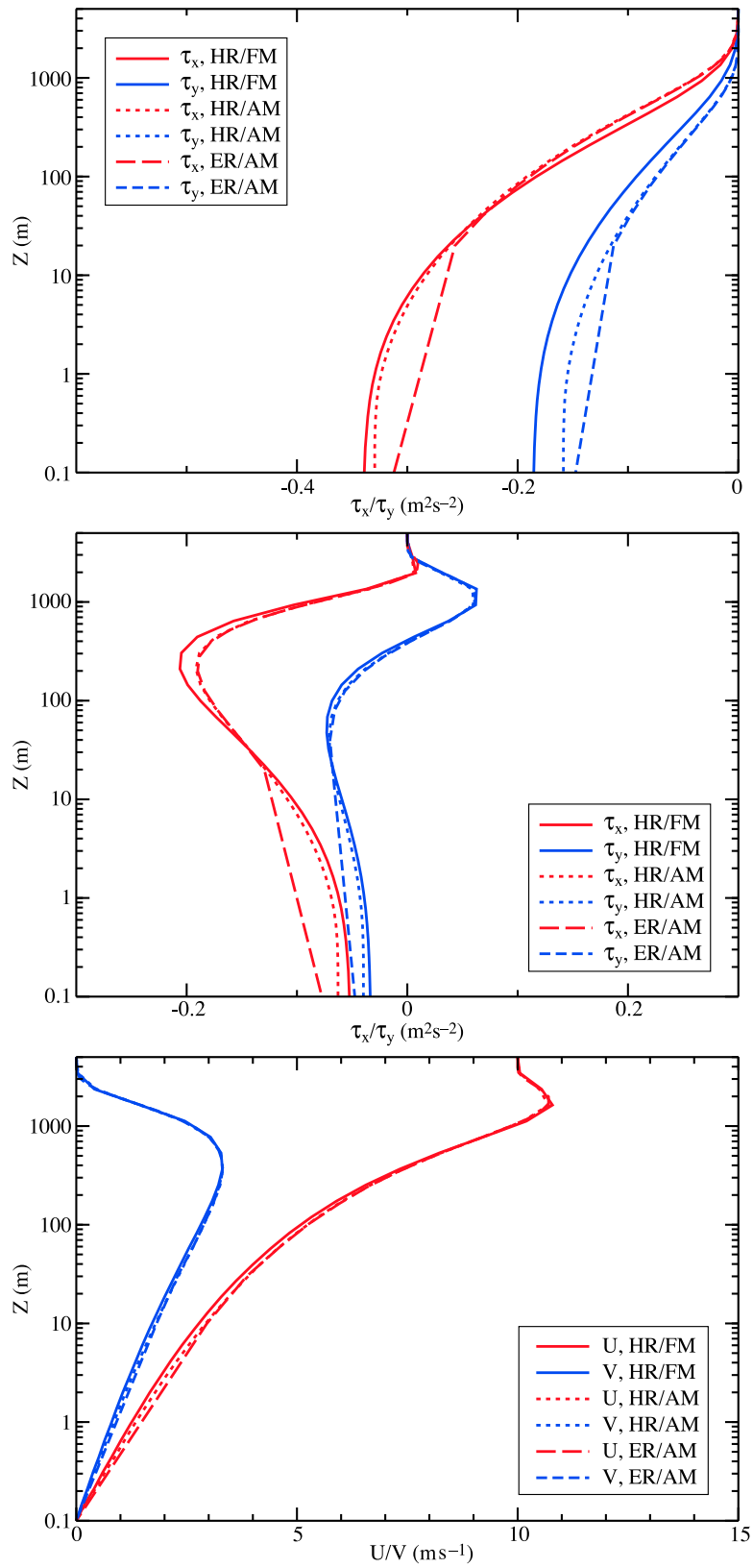


Figure 10: Orographic stress, turbulent stress, and wind profiles for $\sigma_{flt} = 200 \text{ m}$ and $z_o = 0.1 \text{ m}$ with the high resolution full model (HR/FM), the high resolution approximated model (HR/AM) and the ECMWF resolution approximated model (ER/AM).

Two different roughness lengths are used (0.1 and 1 m) with a series of values for σ_{flt} to change the magnitude of the orographic drag. Figure 8 shows the orographic drag coefficient ($|\tau_{os}|/\rho U_G^2$) and the turbulent drag coefficient ($|\tau_{ts}|/\rho U_G^2$) as a function of the amplitude of standard deviation σ_{flt} with HR/FM and HR/AM. The correction coefficient is set to 0.6 for an optimal match of the approximation for a range of parameters. From Fig. 8 it can be seen that the orographic drag coefficient increases with the amplitude of the subgrid orography and that the turbulent drag coefficient decreases. The reason is that with increased orographic drag, the near surface wind decreases and therefore the turbulent surface drag decreases. Figure 9 shows the ageostrophic angle from the single column computations. For high σ_{flt} it increases to above 45 degrees.

The orographic stress, turbulent stress and wind profiles are shown in Fig. 10 for $\sigma_{flt} = 200$ m and $z_o = 0.1$ m. The approximated (HR/AM) and reduced resolution approximated (ER/AM) models are not perfect but follow the full high resolution model (HR/FM) fairly well. The resolution effects are predominantly in the lowest 60 m where the resolution differences are most prominent. Most of the divergence of the orographic stress is in the layer from 10 to 1000 m. It is reassuring that the contribution from the layer below 10 m is fairly small. A significant flux divergence below 10 m would be difficult to resolve in an operational NWP model.

From the surface stress and profile results it can be concluded that the approximated model works fairly well and that the ECMWF resolution does not degrade the results substantially. The errors are non-negligible, but probably small compared to the errors due to uncertainty in the characterization of the global orography in a NWP model.

5 Summary of the new parametrization

The parametrization developed can be summarized with the following set of equations

$$\frac{\partial}{\partial z} \bar{\tau}_o / \rho = -2\alpha\beta C_{md} C_{corr} |\vec{U}(z)| \vec{U}(z) \int_{k_o}^{k_\infty} \frac{k^2}{l_w} F_o(k) e^{-z/l_w} dk, \quad (17)$$

$$l_w = \min(2/k, 2/k_1),$$

with

$$\begin{aligned} F_o(k) &= a_1 k^{n_1}, \text{ for } k_o < k < k_1, \\ F_o(k) &= a_2 k^{n_2}, \text{ for } k_1 < k < k_\infty, \\ n_1 &= -1.9, n_2 = -2.8, \\ a_1 &= \sigma_{flt}^2 (I_H k_{flt}^{n_1})^{-1}, a_2 = a_1 k_1^{n_1 - n_2}, \\ k_o &= 0.000628 \text{ m}^{-1}, k_1 = 0.003 \text{ m}^{-1}, \\ k_{flt} &= 0.00035 \text{ m}^{-1}, k_\infty = 2\pi c_m / z_o, \\ I_H &= 0.00102 \text{ m}^{-1}, c_m = 0.1, \\ \alpha &= 12, \beta = 1, \\ C_{md} &= 0.005, C_{corr} = 0.6. \end{aligned} \quad (18)$$

The integral of the right hand side of (17) can be pre-computed for different heights, without giving a computational burden. However, with hybrid vertical coordinates (as in the ECMWF model), model level heights vary with surface pressure, and therefore it is more convenient to have an analytical expression. As demonstrated in appendix C, a good approximation of (17) is

$$\frac{\partial}{\partial z} \bar{\tau}_{xo} / \rho = -\alpha\beta C_{md} C_{corr} |\vec{U}(z)| \vec{U}(z) 2.109 e^{-(z/1500)^{1.5}} a_2 z^{-1.2}, \quad (19)$$

The use of (19) rather than (17) gives virtually identical results in single column simulations.

The two components of the stress divergence are included in the momentum equations and solved together with the turbulent diffusion equations. An implicit formulation is needed for stability. The standard way of time stepping a non-linear problem with implicit equations is by evaluating the non-linear part at the old time level and keeping the linear part for the new time level. In this case it means that the absolute wind speed $|U|$ is taken from the old time level and that the $U(z)$ and $V(z)$ components are evaluated implicitly. This is exactly the procedure that is already used in the ECMWF model for low level blocking due to scales larger than 5 km (Lott and Miller 1996) and has proven to be numerically robust.

With (19), and the constants in (18), the entire parametrization depends on a single geographical parameter namely the standard deviation of the filtered orography σ_{ft} .

6 Conclusions

A new parametrization for turbulent orographic form drag has been developed. It is based on the work of WM93 in which the orographic surface drag is parametrized for sinusoidal hills and on the suggestion by WBH01 to distribute this drag explicitly in the vertical. It is further inspired by the notion that fine scale data sets with sufficient horizontal resolution to compute slope or silhouette parameters on a global scale, are not available. Therefore the orographic spectrum is parametrized and the effect of all the scales is obtained by integrating over the spectrum.

In order to be practical in an NWP modelling context (for which an implicit numerical treatment is essential), it was necessary to apply rather drastic simplifications, but it is felt that the approximations and simplifications lead to errors that are small compared to the characterization errors of the orography. Although spectral parameters of subgrid orography vary substantially from one location to another, it is felt that the current parametrization is a step forward compared to the traditional effective roughness length concept for a number of reasons (some of which have already been discussed and highlighted by WBH01).

First of all, the entire spectrum of relevant scales is taken into account, in contrast to the common practice of deriving slope parameters from what is available even if the resolution is poor. Changes to the resolution of orographic data have in the past led to changes in slope parameters of factors 3 to 5 in the ECMWF system (Uhrner 2001), which is rather unsatisfactory. In the current parametrization, we use a parameter (σ_{ft}), which is defined in such a way that it can be measured from the available data at 1 km resolution.

Secondly, the convergence problem associated with the variance of the slope not converging when computed as the integral over the spectrum, has been alleviated. This is achieved by including the wind forcing level in the spectral integral. Physically, it means that smaller horizontal scales have a wind forcing at a lower level than the large horizontal scales.

Thirdly, compensation of the roughness lengths of heat and moisture for the orographic enhancement of the aerodynamic roughness is not necessary any more, because the orographic drag is implemented as a separate term in the momentum equations.

Finally, the scheme will interact with boundary layer stability in a completely different way. There is evidence that the effective roughness length scheme in the ECMWF model interacts very strongly with boundary layer stability (Beljaars 2001), and it seems likely that the new scheme with its distributed drag will be less modulated by stability. To find out whether this is realistic will require further research as at this stage there are only very few studies addressing the effects of stability on turbulent form drag (Belcher and Wood 1996; Brown and Wood 2003). In any event, the distributed drag implementation should provide a more flexible framework in



which to take advantage of further advances in understanding in this area.

The new parametrization has clear advantages compared to "effective roughness lengths". The effective roughness length as a concept is appropriate in the sense that it provides a model with the correct drag by definition. However, it may be difficult to define the wind forcing level in case of a wide range of scales and the corresponding logarithmic wind profile near the surface will be in error. However, it is fair to say that ground truth on form drag in real complex terrain is very limited. In order to obtain absolute calibration of drag schemes it will be necessary to have fine scale simulations for a variety of cases with real complex terrain.

APPENDIX

A Standard deviation of small scale orography

To estimate the spectral parameters from the 1 km global data, a band pass filter is applied and the standard deviation of the terrain height is computed from the filtered field. The band pass filter is obtained by using the following smoothing operator two times with different smoothing scales.

$$\begin{aligned}
 h(r) &= \frac{1}{\Delta}, & \text{for } |r| < \Delta/2 - \delta, \\
 h(r) &= \frac{1}{2\Delta} + \frac{1}{2\Delta} \cos \pi(r - \Delta/2 + \delta)/2\delta, & \text{for } \Delta/2 - \delta < |r| < \Delta/2 + \delta, \\
 h(r) &= 0, & \text{for } |r| > \Delta/2 + \delta.
 \end{aligned} \tag{A.1}$$

This smoothing operator is a top hat function with smooth edges. The edges reduce the amplitude of the side lobes in the spectral domain. The filter is applied by convoluting the input field in two dimensions with $h(r)$, where r is the radial distance. Parameter Δ is the width of the filter and δ is the width of the edge. Sardeshmukh and Hoskins (1984) show that a rotation symmetric smoothing is equivalent to filtering of the total wavenumber. The effect of this operation is equivalent to multiplying the spectrum by a filter function $H(k)$ where H is the square of the Fourier transform of $h(r)$.

To compute the standard deviation of the small scale orography for well defined scales all over the globe (also in polar regions where the grid point spacing is much less than 1 km), the 30" field is filtered twice with filter (A.1). The first time, the smallest scales are filtered out by using $\Delta_1 = 2$ km and $\delta_1 = 1$ km. The second filtering is done with $\Delta_2 = 20$ km and $\delta_2 = 1$ km, to isolate the longer scales. The standard deviation of the difference of the two fields is computed on a 2' 30" grid. The advantage of this procedure is that the computed orographic standard deviation represents the same scale all over the globe, i.e. also in polar regions.

The spectral filter for the small scale orography corresponding to the procedure described above is

$$\begin{aligned}
 H_{flt}(k) = & \frac{1}{\Delta_1^2} \left\{ \frac{\sin(k\Delta_1/2 - k\delta_1)}{k} + \frac{\sin(k\Delta_1/2 + k\delta_1)}{k} \right. \\
 & \left. + \frac{\cos(\pi/2 + k\Delta_1/2) \sin(\pi/2 + k\delta_1)}{\pi/(2\delta_1) + k} + \frac{\cos(\pi/2 - k\Delta_1/2) \sin(\pi/2 - k\delta_1)}{\pi/(2\delta_1) - k} \right\}^2 \\
 & - \frac{1}{\Delta_2^2} \left\{ \frac{\sin(k\Delta_2/2 - k\delta_2)}{k} + \frac{\sin(k\Delta_2/2 + k\delta_2)}{k} \right. \\
 & \left. + \frac{\cos(\pi/2 + k\Delta_2/2) \sin(\pi/2 + k\delta_2)}{\pi/(2\delta_2) + k} + \frac{\cos(\pi/2 - k\Delta_2/2) \sin(\pi/2 - k\delta_2)}{\pi/(2\delta_2) - k} \right\}^2.
 \end{aligned} \tag{A.2}$$

The filter of (A.2) is shown in Fig. A.2. The filter has the shape of a band pass filter with the lower bound determined by Δ_2 , and the upper bound by Δ_1 . Parameters δ_1 and δ_2 control the level of overshooting. The parameter selection is based on the following ideas. First the filter should drop off quickly near $k = 0.0012 \text{ m}^{-1}$ (see Fig. 1), because we want to delete the aliasing tail of the spectrum (the 30" data has the aliasing tail a factor 10 lower than the 3" data in Fig. 1, see Uhrner 2001). Secondly we would like to cut off below scales of 5 km because this is the resolution of the 2' 30" grid on which the standard deviation will be computed. However, this leads to a very narrow filter and therefore we select a longer filtering scale of about 20 km. The edges of the filter defined by $H_{flt} = 0.0005$ are $k = 0.00014 \text{ m}^{-1}$ and $k = 0.00112 \text{ m}^{-1}$ respectively. These wave numbers correspond to length scales (half wave length) of 22000 m and 3000 m. The result of this filtering is

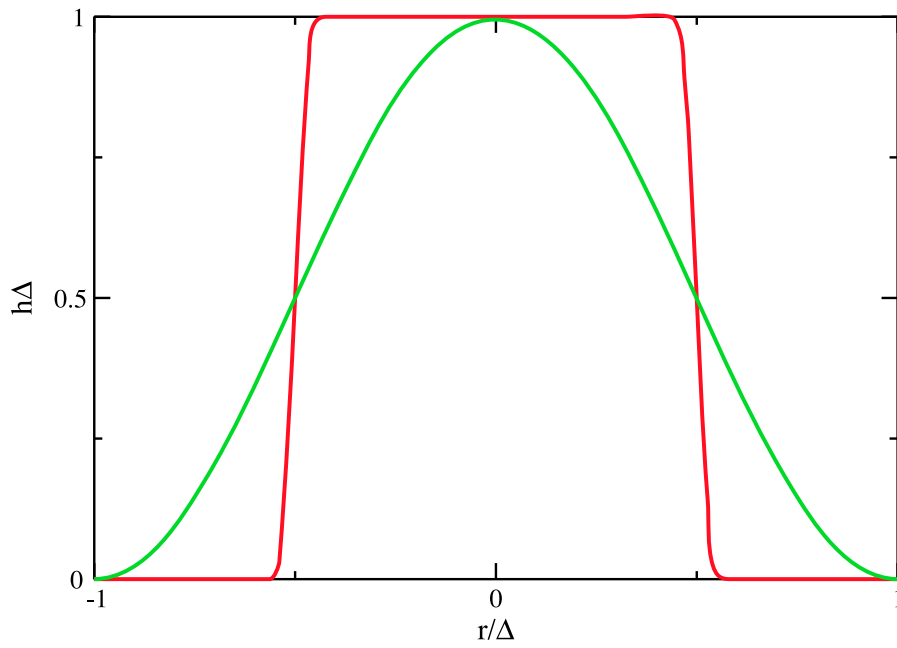


Figure A.1: Smoothing operators for $\delta = \Delta/20$ (solid), and $\delta = \Delta/2$ (dashed).

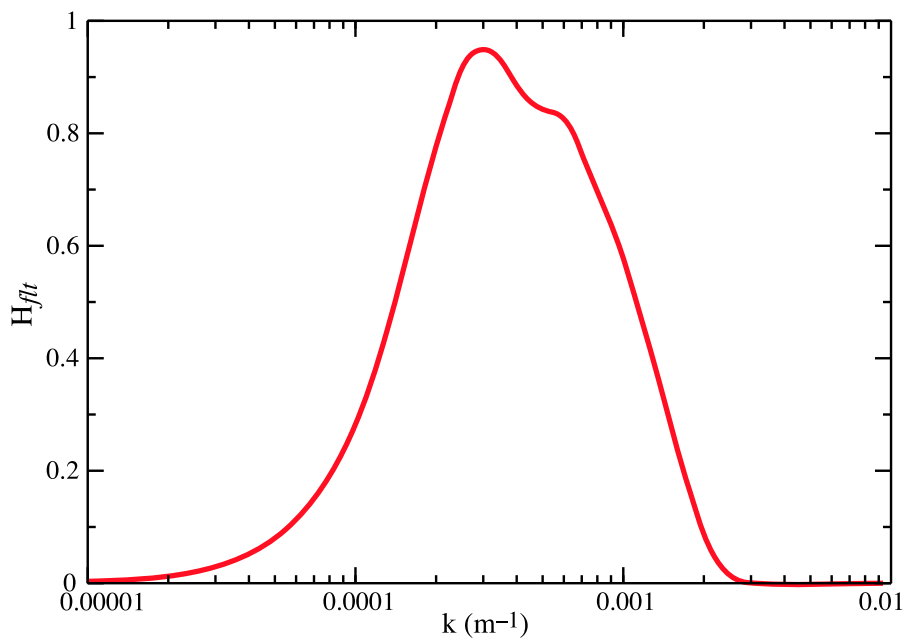


Figure A.2: Spectral filter corresponding to difference of two smoothing operations with: $\Delta_1 = 2000$ m, $\Delta_2 = 20000$ m, $\delta_1 = 1000$ m, $\delta_2 = 1000$ m.

that the computed standard deviation on the 2' 30" grid will not really have a resolution of 5000 m, but it will be smooth with smallest represented scales of about 22000 m. The advantage of having a broad filter is that resulting standard deviations will be less noisy. In the ECMWF system, the 2' 30" fields are further averaged to the target resolution of the different model versions (e.g. 40 km for the operational deterministic model).

With an orography spectrum F_o and the band pass filtering with (A.2), the following spectrum is obtained for the small scale orography

$$F_{flt}(k) = F_o(k)H_{flt}(k). \quad (\text{A.3})$$

The variance of the sub-grid orography as computed from the filtered fields is

$$\sigma_{flt}^2 = \int F_o(k)H_{flt}(k)dk \quad (\text{A.4})$$

$$\approx F_o(k_{flt}) \int H_{flt}(k)dk \quad (\text{A.5})$$

$$= F_o(k_{flt})I_H. \quad (\text{A.6})$$

The approximation is based on the idea that the band width of the filter is small and that the spectrum of the orography does not change much over the band width of the filter. So, by computing the variance of the small scale orography σ_{flt}^2 , an estimate is obtained of the orographic power spectrum at wavelength k_{flt} :

$$F_o(k_{flt}) = \sigma_{flt}^2/I_H. \quad (\text{A.7})$$

For a power spectrum with exponent n_1 in the range of the band filter, a filter wave number can be defined that satisfies (A.6) exactly

$$k_{flt}^{n_1} = \left\{ \int k^{n_1} H(k) dk \right\} \left\{ \int H(k) dk \right\}^{-1}. \quad (\text{A.8})$$

With the filter parameters $\Delta_1 = 2000$ m, $\delta_1 = 1000$ m, $\Delta_2 = 20000$ m, $\delta_2 = 1000$ m, and $n_1 = -1.9$, the following results are found from numerical integration:

$$I_H = 0.00102 \text{ m}^{-1}, \quad k_{flt} = 0.00035 \text{ m}^{-1}. \quad (\text{A.9})$$

B Single column model

The single column model that is used in this paper consists of the Ekman equations with a simple turbulence closure for neutral situations and subgrid orographic stress terms as formulated in (12) and (13) respectively. The equations are

$$\frac{\partial U}{\partial t} = f(V - V_G) + \frac{\partial}{\partial z} K \frac{\partial U}{\partial z} + \frac{1}{\rho} \frac{\partial \tau_{xo}}{\partial z}, \quad (\text{B.1})$$

$$\frac{\partial V}{\partial t} = -f(U - U_G) + \frac{\partial}{\partial z} K \frac{\partial V}{\partial z} + \frac{1}{\rho} \frac{\partial \tau_{yo}}{\partial z}, \quad (\text{B.2})$$

where U_G and V_G are the two components of the geostrophic wind, f is the Coriolis parameter, K the eddy diffusion coefficient, and τ_{xo} and τ_{yo} are the two components of the orographic stress. Since only neutral flow

is considered here, the eddy diffusivity formulation can be very simple. The standard mixing length scheme is selected with the Blackadar asymptotic mixing length

$$K = l^2 \left| \frac{d\vec{U}}{dz} \right|, \quad (\text{B.3})$$

$$l^{-1} = (\kappa z)^{-1} + \lambda^{-1}, \quad \lambda = 150 \text{ m}, \quad (\text{B.4})$$

The orographic stress divergence terms are represented either by the full (12) or by its approximation (13). For simplicity, density, ρ , is set to 1.

For the vertical grid two different resolutions are used: (i) a High Resolution grid with 30 grid points logarithmically distributed between the specified roughness length and 5000 m (HR), and (ii) the ECMWF operational Resolution with 23 grid points from 10 m up to 5000 m (ER). The main difference is that HR resolves the layer between the roughness length and 60 m better than ER.

The equations are solved numerically with an implicit solver for the linear terms. The time step is 10 minutes. The integrals are evaluated every time step with standard library routines using Romberg's method (Press et al. 1986).

C Approximation of the spectral integral

The right hand side of (13) contains the integral

$$I_R = 2 \int_{k_o}^{k_\infty} \frac{k^2}{l_w} F_o(k) e^{-z/l_w} dk, \quad (\text{C.1})$$

with $l_w = \min(2/k, 2/k_1)$,

which is a function of z . The upper bound of the integral has been replaced by $k_\infty = 2\pi c_m/z_o$, because for higher wave numbers the corresponding wind forcing level would be below the surface. The orographic spectrum is assumed to have a power law shape in two different regimes with parameters according to (18).

In a large scale model it is convenient to have an analytical expression of this integral rather than having to do numerical integration. To find an approximate expression for I_R , first consider small z for which the integral is dominated by high wave numbers, so that $l_w = 2/k$ is used and the high wave number part of (18) is:

$$I_{RI} = \int_{k_1}^{\infty} a_2 k^{3+n_2} e^{-zk/2} dk. \quad (\text{C.2})$$

The solution is (Gradsteyn and Ryznik 1980, p. 317 and p. 941)

$$I_{RI} = a_2 (z/2)^{-4-n_2} \Gamma(4+n_2, k_1 z/2), \quad (\text{C.3})$$

where Γ is the incomplete gamma function. An approximation for small z with $n_2 = -2.8$ is

$$\begin{aligned} I_{RI} &= a_2 (z/2)^{-4-n_2} \Gamma(4+n_2), \\ &= a_2 (z/2)^{-1.2} \Gamma(1.2) = a_2 2.297 z^{-1.2} 0.9182 = 2.109 a_2 z^{-1.2}, \end{aligned} \quad (\text{C.4})$$

where Γ is the gamma function ($\Gamma(1.2) = 0.9183$, see Abramowitz and Stegun, 1970). This approximation turns out to give a nearly perfect match in the height regime from about $10z_o$ to 500 m above the surface. In order to get a good fit for all z , an empirical correction is applied which leads to the following approximation

$$I_R = 2.109 e^{-(z/1500)^{1.5}} a_2 z^{-1.2}. \quad (\text{C.5})$$

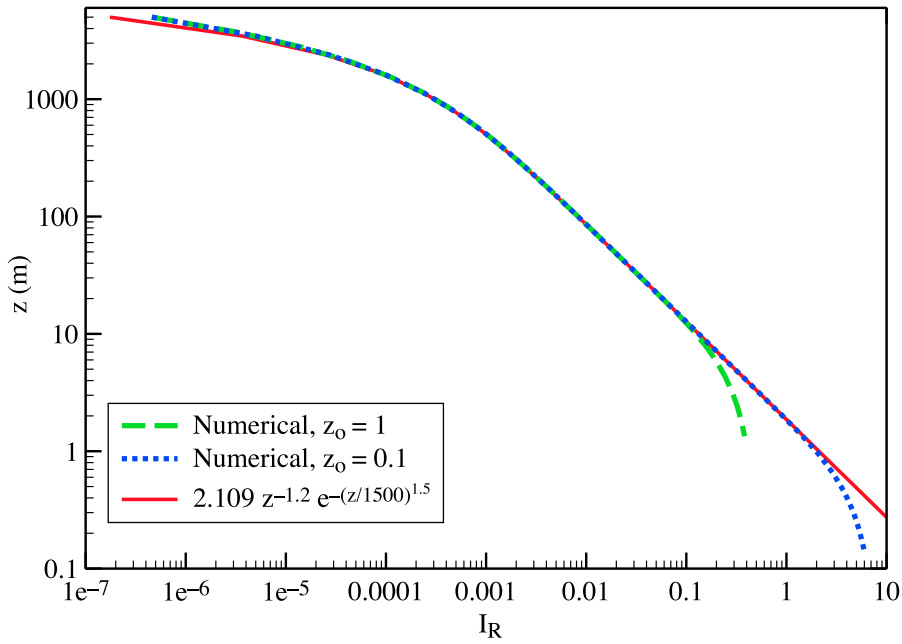


Figure C.1: Integral in (C.1) as a function of z , evaluated numerically and from approximation $2.109 * z^{-1.2} \exp(-(z/1500)^{1.5})$.

Figure (C.1) shows I_R as a function of z from numerical integration compared to (C.5). The match is nearly perfect except near the surface where the upperbound of the integral ($k_\infty = 2\pi c_m/z_0$) plays a role. However, this approximation will be used on model levels only, i.e. not below 10 m.

Acknowledgements

The authors would like to thank Peter Taylor for extensive discussions on the subject and suggesting that the convergence problem of the variance of slope might be related to a scale dependent wind forcing. We also would like to thank Peter Janssen for his assistance in finding approximations of the spectral integrals.

References

- Abramowitz, M. and Stegun, I.A. (1970): *Handbook of mathematical functions*, Dover Publications, New York.
- Bannon, P.R. and Yuhas, J.A. (1990): On mountain wave drag over complex terrain, *Meteor. Atmos. Phys.*, **43**, 155-162.
- Belcher, S.E., Newley T.M.J. and Hunt, J.C.R. (1993): The drag on an undulating surface induced flow of a turbulent boundary layer, *J. Fluid Mech.*, **249**, 557-596.
- Belcher, S.E. and Wood, N. (1996): Form and wave drag due to stably stratified turbulent flow over low ridges, *Quart. J. Roy. Meteor. Soc.*, **122**, 863-596.

- Beljaars, A.C.M. (2001): Issues in boundary layer parametrization for large scale models, in: *Issues in parametrization of subgrid processes*, ECMWF seminar proceedings, Reading, England.
- Brown, A.R. and Wood, N. (2003): The stable boundary layer over moderate topography, *J. Atmos. Sci.*, **60**, 2797-2808.
- ECMWF (1997): *Proceedings of a workshop on orography*, ECMWF, Reading, England.
- Gesch, D.B. and Larson, K.S. (1998): Techniques for development of global 1-kilometer digital elevation models, in: *Proceedings, Pecora Thirteen Symposium*, Sioux Falls, South Dakota, August 20-22, 1996 (CD-ROM), Am. Soc. for Photogrammetry and Remote Sensing, Bethesda, Md.
- Gradsteyn, I.S. and Ryznik, I.M. (1980): *Table of integrals, series, and products*, Academic Press.
- Grant, A.L.M. and Mason, P.J. (1990): Observations of boundary layer structure over complex terrain, *Quart. J. Roy. Meteor. Soc.*, **116**, 159-186.
- Hara, T. and Belcher, S.E. (2002): Wind forcing in the equilibrium range of wind-wave spectra, *J. Fluid Mech.*, **470**, 223-245.
- Hewer, F. and Wood, N. (1998): The effective roughness length for scalar transfer in neutral conditions over hilly terrain, *Quart. J. Roy. Meteor. Soc.*, **124**, 659-685.
- Lott, F. and Miller, M.J. (1996): A new subgrid-scale orographic drag parametrization: Its formulation and testing, *Quart. J. Roy. Meteor. Soc.*, **123**, 101-127.
- Mason, P.J. (1985): On the parametrization of orographic drag, In: *Physical parametrization for numerical models of the atmosphere*, ECMWF seminar proceedings, Reading, England.
- Mason, P.J. (1991): Boundary layer parametrization in heterogeneous terrain, In: *Fine-scale modelling and the development of parametrization schemes*, ECMWF workshop proceedings, Reading, England.
- Mengesha, Y.G., Taylor, P.A. and Lenschow, D.H. (2001): Boundary-layer turbulence over the Nebraska Sandhills, *Bound.-Layer Meteor.*, **100**, 3-46.
- Milton, S.F. and Wilson, C.A. (1996): The impact of parametrized subgrid-scale orographic forcing on systematic errors in a global NWP model, *Mon. Weather Rev.*, **124**, 2023-2045.
- Press, W.H., Flannery, B.P., Teukolsky, S.A. and Vetterling, W.T. (1986): *Numerical recipes: The art of scientific computing*, Cambridge University Press.
- Sardeshmukh, P.D. and Hoskins, B.J. (1984): Spatial smoothing on the sphere, *Month. Wea. Rev.*, **112**, 2524-2529.
- Taylor, P.A., Sykes, R.I. and Mason, P.J. (1989): On the parameterization of drag over small-scale topography in neutrally-stratified boundary-layer flow, *Bound.-Layer Meteor.*, **48**, 408-422.
- Uhrner, U. (2001): *The impact of new sub-grid scale orography fields on the ECMWF model*, ECMWF Technical Memo nr. 329.



Wood, N., Brown, A.R. and Hewer, F.E. (2001): Parametrizing the effects of orography on the boundary layer, an alternative to effective roughness lengths, *Quart. J. Roy. Meteor. Soc.*, **127**, 759-778.

Wood, N. and Mason, P.J. (1993): The pressure force induced by neutral, turbulent flow over low hills, *Quart. J. Roy. Meteor. Soc.*, **119**, 1233-1267.

Young, G.S. and Pielke, R.A. (1983): Application of terrain height variance spectra to mesoscale modelling, *J. Atmos. Sci.*, **40**, 2555-2560.